eXPRESS Polymer Letters Vol.2, No.9 (2008) 630–638
Available online at www.expresspolymlett.com
DOI: 10.3144/expresspolymlett.2008.76

Studies of structural, thermal and electrical behavior of polymer nanocomposite electrolytes

Dillip K. Pradhan, R. N. P. Choudhary, B. K. Samantaray*

Department of Physics and Meteorology, Indian Institute of Technology, Kahargapur-721302, India

Received 19 June 2008; accepted in revised form 27 July 2008

Abstract. Structural, thermal and electrical behavior of polymer-clay nanocomposite electrolytes consisting of polymer (polyethylene oxide (PEO)) and NaI as salt with different concentrations of organically modified Na^+ montmorillonite (DMMT) filler have been investigated. The formation of nanocomposites and changes in the structural properties of the materials were investigated by X-ray diffraction (XRD) analysis. Complex impedance analysis shows the existence of bulk and material-electrode interface properties of the composites. The relative dielectric constant (ε_r) decreases with increase in frequency in the low frequency region whereas frequency independent behavior is observed in the high frequency region. The electrical modulus representation shows a loss feature in the imaginary component. The relaxation associated with this feature shows a stretched exponential decay. Studies of frequency dependence of dielectric and modulus formalism suggest that the ionic and polymer segmental motion are strongly coupled manifeasting as peak in the modulus (M'') spectra with no corresponding feature in dielectric spectra. The frequency dependence of ac (alternating current) conductivity obeys Jonscher power law feature in the high frequency region, where as the low frequency dispersion indicating the presence of electrode polarization effect in the materials.

Keywords: *nanocomposites, X-ray diffraction, ac conductivity, conductivity relaxation*

1. Introduction

The combination of clay and functional polymers interacting at atomic level constitute the basis for preparing an important class of inorganic-organic nanostructured materials i.e., polymer nanocomposites [1, 2]. Among these nanocomposites, the intercalation of electroactive species into the interlayer spacing of 2:1 phyllosilicate (such as montmorillonite, hectorite, laponite etc.) is a method to construct a novel hybrid supermolecular assembly with particular electrical behavior [1–5]. Intercalation of polymers, in principle, leads to the formation of new materials, which combine the optical and electrical properties of the polymer with mechanical strength, thermal stability etc. of the inorganic host and so possesses properties which may not be achieved by either component separately. Solid polymer electrolytes (SPEs) formed by complexing alkali metal salts with polyethers such as polyethylene oxide (PEO) have widely been studied for potential applications in solid state batteries and other electrochemical devices [6–8]. They are also of fundamental interest because of their unusual mechanism of ionic transport, which they exhibit and for which a detailed understanding is still lacking [8]. It is now well established that significant ionic motion occurs only in the elastomeric amorphous phase of the polymer and is closely associated with the segmental motion of polymers [8]. Measurement and analysis of SPEs are complicated by various factors. First these materials are often heterogeneous with both amorphous and crystalline regions and the distribution of salt concentration may vary throughout the poly-

*Corresponding author, e-mail: crnpfl@phy.iitkgp.ernet.in

mer electrolyte [9]. Second at certain salt concentrations (where significant coupling occurs), there is an anionic contribution to the conductivity [10]. Moreover because of the low dielectric constant of PEO, polymer mediated cation anion pair formation is unavoidable [11]. The intercalated polymer nanocomposite electrolytes (PNCEs) are attractive because the bulky anions cannot enter into the nanometric gallery of the layered silicate (such as montmorillonite, hectorite, laponite etc.), whereas the polymer and cation can enter into that nanometric channel of the clay. Hence the formation of cation anion pair and dual ionic conduction are expected to be minimum. These PNCEs, in principle, therefore provide the opportunity to investigate conductivity and associated relaxation in polymer electrolyte free from previously mentioned problems. We have used here montmorillonite (MMT) clay as inorganic filler, which possesses intercalation property. The filler is organically modified with dodecyl amine so that the hydrophilic nature of the silicate layer is changed into hydrophobic, and the interlayer spacing expands. Indeed this creates appropriate environment for the intercalation of polymer chains between clay layers [12]. Though there has been a considerable amount of work performed on synthesis and characterization of PNCEs (polymer-layered silicate nanocomposite electrolytes) by various research groups [1–5, 12, 13], not much work has been reported on dielectric and electrical properties of PNCEs as yet.

In view of the above, the present paper aims to report structural, thermal and electrical behavior of an ionicallly conducting polymer nanocomposites system: $(PEO)_{25}$-NaI + *x* wt% DMMT with different values of *x*. The effect of DMMT (i.e., dodecyl amine modified MMT) concentration on electrical and ac conductivity response has been investigated in order to gain better understanding of ion transport behavior in PNCEs.

2. Experimental details

Polymer-clay nanocomposite electrolytes [$(PEO)_{25}$-NaI + *x* wt% DMMT (*x* = 0,5, 10, 15, 20, 30, 50)] consist of polymer, polyethylene oxide (PEO) with molecular weight of $6 \cdot 10^5$ (M/S Aldrich, USA) and NaI (M/S Merck India Ltd, Mumbai, India) as salt with different concentrations of DMMT (MMT supplied by University of Missouri, Coulambia, USA) have been synthesized by a tape casting technique using the self designed tape caster. The PEO and sodium salt molar ratio was maintained at 25:1 (i.e., $(PEO)_{25}$-NaI). It means that the there is sufficient number of available sites (i.e., the oxygen atoms in PEO) for Na-ion to hop from one site to another one. Detailed preparation and characterization methods for similar type of systems have already been reported [14, 15]. The X-ray diffraction pattern of the PNCEs films was recorded at room temperature using an X-ray powder diffractometer (Rigaku Miniflex) with CuK_α radiation ($\lambda = 0.15405$ nm) in 2θ (Bragg angles) range ($2° \leq 2\theta \leq 10°$) at a scan speed of 0.5°/min. Thermogravimetric (TG) analysis was performed using a SHIMADZU thermogravimetric analyzer. Samples were heated in a platinum pan from room temperature to 600°C at a heating rate of 10°C/min under nitrogen atmosphere. An analysis of the electrical behavior of PNCE films was carried out using impedance spectroscopy on the application of a small ac signal (100 mV) across the symmetrical cell of the type SS||PNCE||SS (where SS stands for stainless steel blocking electrodes). Complex impedance parameters (i.e., impedance, phase angles, permittivity and tangent loss parameters) were obtained by a computer-controlled impedance analyzer (HIOKI LCR Hi-Tester, Model:3532, Japan) as a function of frequency (100 Hz to 1 MHz) at different temperatures (30 to 150°C). The ac conductivity was evaluated from dielectric data in accordance with the relation: $\sigma_{ac} = \omega \varepsilon_0 \varepsilon_r \tan\delta$ where $\varepsilon_r = C/C_0$ is the relative permittivity, $\tan\delta$ = loss tangent, C_0 = vacuum capacitance of the cell. The real and imaginary parts of impedance, permittivity and electric modulus were calculated using Equations (1)–(5):

$$Z^* = Z' - jZ'' \tag{1}$$

$$\varepsilon^* = \varepsilon' - j\varepsilon'' \tag{2}$$

where

$$\varepsilon' = \frac{-Z''}{\omega C_0 (Z'^2 + Z''^2)} \tag{3}$$

$$\varepsilon'' = \frac{Z'}{\omega C_0 (Z'^2 + Z''^2)} \tag{4}$$

and

$$M^* = M' + jM'' = \frac{1}{\varepsilon^*} = j\omega\varepsilon_0 Z^* \quad (5)$$

3. Results and discussion

3.1. X-ray diffraction

XRD studies have been carried out in order to monitor the formation of the nanocomposites. Figure 1 shows the XRD patterns of Na^+-MMT, DMMT and $(PEO)_{25}$-NaI +x wt% DMMT for different values of x at room temperature in the range of 3–10°. The peaks were assigned to the 001 basal reflection of DMMT. It is observed that Na^+-MMT exhibits (001) reflection peak at an angle ($2\theta = 7.27°$) corresponding to the interlayer spacing (d_{001}) 1.215 nm. Upon modification with dodecyl amine, the peak shifts toward the lower angle side corresponding to interlayer spacing of 1.568 nm, indicating the successful intercalation of alklyl ammonium ion into the gallery of MMT. When DMMT is added to polymer salt complex, there is an increase in the d_{001} (i.e., the peak position of (001) plane shift towards the lower angle side), which indicates that there is an increase in the gallery height. This suggests the successful intercalation of polymer-salt complex into the nanometric gallery of the DMMT confirming the formation of nanocomposites [16].

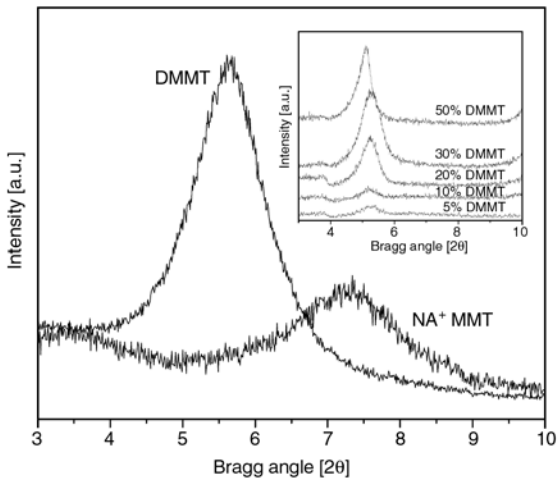

Figure 1. Comparison of XRD patterns of Na^+-MMT, DMMT and $(PEO)_{25}$-NaI + x wt% DMMT with different concentrations of DMMT (x)

3.2. Thermogravimetric analysis

Figure 2 shows the TGA curves of $(PEO)_{25}$-NaI + x wt% of DMMT with different value of x. For both, the polymer-salt complexes and PNCEs, a small amount of mass loss at low temperatures (T<125°C) is assigned to elimination of water or residual solvent (if any). For x = 0 (i.e., polymer-salt complex), a sharp mass loss occurs corresponding to the decomposition of PEO after the elimination of water. It has been established [17] that the volatile evolution of both PEO and polymer-salt complexes occurs in a single step after elimination of water, while the complex leaves a residual quantity above 500°C. In addition to this sharp weight loss, another broad weight loss occurs at higher temperatures for PNCEs. It is generally assumed [18], that in intercalated PNCEs materials, some PEO chains reside inside the gallery and others outside the gallery. So the sharp weight loss is expected due to the PEO chains residing outside the gallery. The broad loss (at higher temperatures) is attributed to the decomposition of PEO inside the gallery since no weight loss for DMMT is observed in the same temperature range. PEO chains inside the silicate gallery are responsible for broader weight loss, as the degradation products need more temperature to depart from the silicate gallery. From the Figure 2, it is observed that on addition of small amount of clay the (residual) weight loss increases because of the restriction of thermal motion of the polymer in the silicate layer. Again, the residual weight loss increases on increasing DMMT concentration.

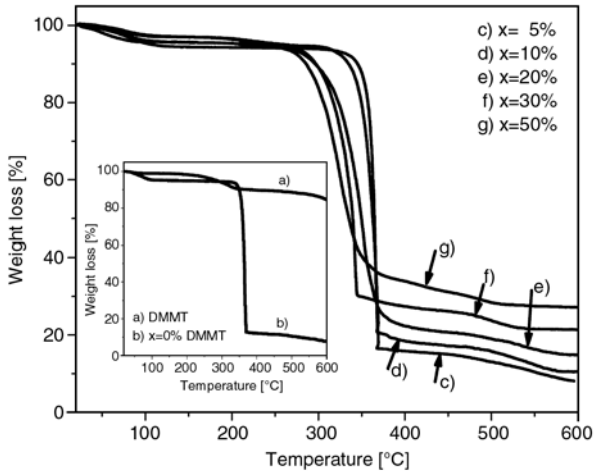

Figure 2. TGA thermograms of DMMT (a) and PNCEs films of $(PEO)_{25}$-NaI + x wt% of DMMT with different values of x, i.e., x = 0% (b), x = 5% (c), x = 10% (d), x = 20% (e), x = 30% (f) and x = 50% (g)

3.3. Complex impedance spectroscopy

Figure 3 represents the complex impedance spectrum/Nyquist plot (Z'' vs. Z') of PNCE films of $(PEO)_{25}$-NaI + x wt% of DMMT for various clay concentrations (x) at room temperature. The typical Nyquist plot of the samples comprises of a broadened semicircle in the high frequency region followed by a tail (spike) in the lower frequency region. The higher frequency semicircle can be ascribed mainly to the bulk properties of the materials, where as the low frequency spike indicates the presence of double layer capacitance at the electrode/sampleinterface [19]. The intercept of the semicircle with the real axis (Z') at low frequency (end) give rise to the bulk (ionic) resistance (R_b) of the materials.

Figure 4 shows the temperature dependence of impedance spectra of (a) $(PEO)_{25}$-NaI and (b) $(PEO)_{25}$-NaI + 5 wt% DMMT as a representative plot. It is clear that the diameter of the semicircle of high frequency region decreases with rise in temperature, and finally it vanishes above 60°C, leaving only a spike in the spectrum. The presence of semicircle signifies the persistence of capacitance associated with the heterogeneity textures of the composites. The polymer electrolytes are heterogeneous due to the presence of both amorphous and crystalline regions. The disappearance of the semicircle indicates the homogeneity of the system, which agrees well with the reported one [20]. The change in the diameter of semicircle indicates that R_b decreases with increase of temperature. On the other hand, the slope of the straight line (due to material electrode interface) does not vary significantly with temperature, which indicates that no electrochemical degradation of the electrodes occurs during the conductivity measurement. Similar type of explanation has been reported elsewhere [21] in many other systems.

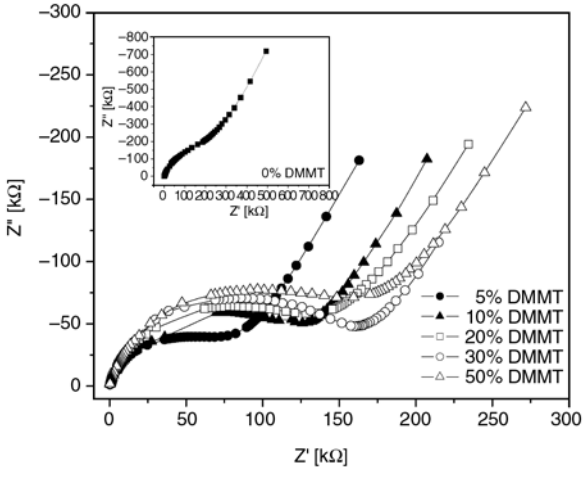

Figure 3. Variation of imaginary (Z'') with real (Z') part of impedance of $(PEO)_{25}$–NaI + x wt% of DMMT with different concentrations (x) of DMMT at room temperature (30°C)

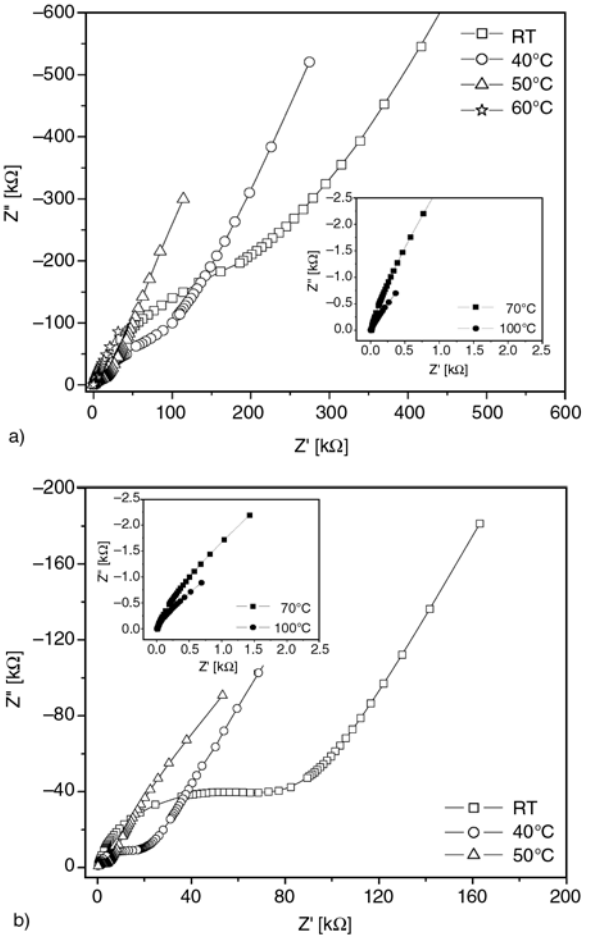

Figure 4. Complex impedance spectrum of (a) $(PEO)_{25}$-NaI and (b) $(PEO)_{25}$-NaI + 5 wt% DMMT as representative at different temperatures

3.4. Dielectric properties

Figure 5 shows the variation of relative dielectric constant (ε_r) with frequency of the PNCE films with varying DMMT concentration at room temperature. In all cases, a strong frequency dispersion of permittivity was observed in the low frequency region followed by a nearly frequency independent behavior above 5 kHz. The decrease of ε_r with increase in frequency is attributed to the electrical relaxation processes, but at the same time the material electrode polarization cannot be ignored, as our samples are ionic conductors. It has been observed

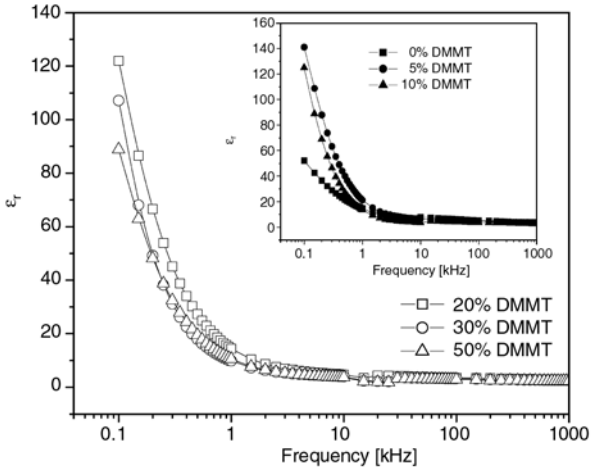

Figure 5. Variation of relative dielectric constant (ε_r) of PNCEs with frequency for different concentrations of DMMT of $(PEO)_{25}$-NaI + *x* wt% DMMT at room temperature (30°C)

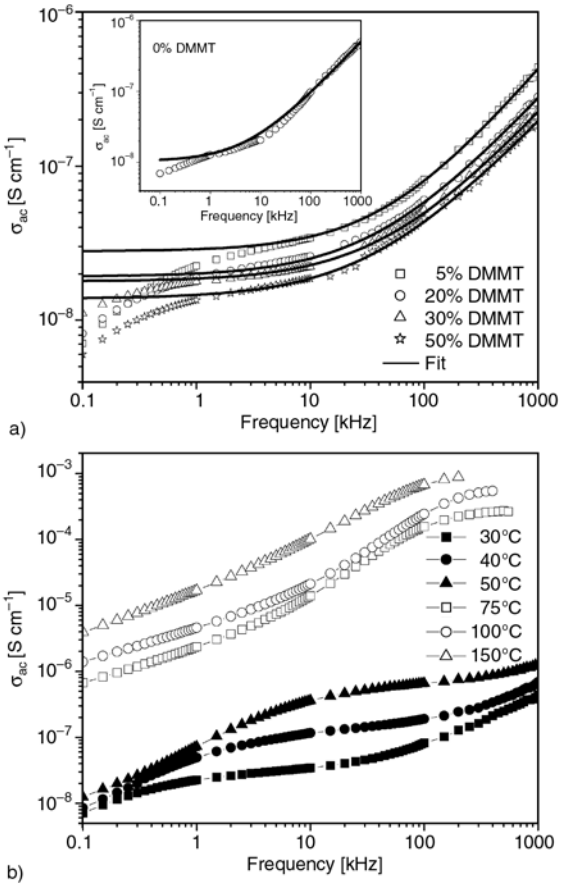

Figure 6. Comparison of frequency dependent ac conductivity of $(PEO)_{25}$-NaI + *x* wt% DMMT for (a) different values of *x* at room temperature (30°C); (b) for *x* = 5% at different temperatures. The continuous solid line represents the fit of experimental to the power law $\sigma(\omega) = \sigma_0 + A\omega^n$.

that the relative permittivity of PNCEs is higher than that of the polymer-salt complex, and the maximum value is found for 5% clay concentration. The enhancement of dielectric properties may be due to the following reasons. The large scale heterogeneity in polymer salt complex is suppressed in the nanocomposite, and is replaced by small scale heterogeneity. The small scale heterogeneity is connected to the presence of silicate layer, which increases the free volume, due to looser segmental packing in chains confined to nanovolume [22].

3.5. AC conductivity

The frequency dependent ac conductivity of $(PEO)_{25}$-NaI + *x* wt% DMMT for (a) different values of *x* at room temperature (30°C) and (b) for *x* = 5% for different temperatures is shown in Figure 6. The ac conductivity patterns show a frequency independent plateau in the low frequency region and exhibits dispersion at higher frequencies. This behavior obeys the universal power law [23, 24], $\sigma(\omega) = \sigma_0 + A\omega^n$, where σ_0 is the *dc* conductivity (frequency independent plateau in the low frequency region), *A* is the pre-exponential factor and *n* is the fractional exponent between 0 and 1 (the solid line is the fit to the expression). The effect of electrode polarization is evidenced by small deviation from σ_{dc} (plateau region) value in the conductivity spectrum (in the low frequency region). With rise in temperatures, the low frequency electrode polarization phenomena become more prominent and thus plateau region shifts to higher frequency side (Figure 6b). The values of σ_0, *A* and *n* obtained by fitting the universal power law are given in Table 1 (for Figure 6a). Generally, for ionic conductors, power law exponents can be between 1 and 0.5 indicating the ideal long-range pathways and diffusion limited hopping (tortuous pathway) respectively [25]. The value of exponent (Table 1) of the higher frequency slopes shows that the long-range drift of ions may be one of the main reasons of ionic conduction [25] in the system. It has been observed that (Table 1) the maximum value of conductivity was found to be $2.8 \cdot 10^{-8}$ S·cm^{-1} for 5% DMMT concentration whereas for higher DMMT concentration the conductivity decreases monotonically (room temperature). This observation can be explained by an empirical Equation (6):

$$\sigma = \sum n_i \mu_i z_i \tag{6}$$

Table 1. Comparison of parameters obtained from fit to the experimental data to $\sigma(\omega) = \sigma_0 + A\omega^n$ and $\Phi = \Phi_0 \exp[(-t/\tau)^\beta]$ functions respectively of $(PEO)_{25}$-NaI +*x* wt% DMMT, for different DMMT concentration (*x*) at room temperature

x [%]	σ_0 [S·cm^{-1}]	A	n	τ [s]	β	M_∞
0	$1.04\cdot10^{-8}$	$1.58\cdot10^{-11}$	0.748	$1.2\cdot10^{-5}$	0.52	0.21
5	$2.80\cdot10^{-8}$	$2.03\cdot10^{-12}$	0.883	$5.3\cdot10^{-5}$	0.57	0.26
10	$2.08\cdot10^{-8}$	$1.31\cdot10^{-12}$	0.887	–	–	–
20	$1.92\cdot10^{-8}$	$3.11\cdot10^{-11}$	0.819	$5.0\cdot10^{-5}$	0.55	0.36
30	$1.78\cdot10^{-8}$	$2.74\cdot10^{-12}$	0.813	$5.5\cdot10^{-5}$	0.56	0.40
50	$1.38\cdot10^{-8}$	$3.45\cdot10^{-12}$	0.787	$5.5\cdot10^{-5}$	0.57	0.42

where n_i, μ_i, and z_i refer to charge carrier, ionic mobility, and ionic charge of i^{th} ion respectively. It is clear from the equation that the conductivity depends on the amount of charge carrier (n_i), and the mobility of the ionic species in the system. Addition of clay can increase the fraction of free ions (i.e., increase of n_i) because the negative charge in the silicate layers can interact with the Na^+ cation and disturb the attractive forces between cation and anion of the salt. When excesses amount of DMMT is added to polymer-salt complex, there may be an increase in the system viscosity and thus restricted cation mobility (i.e., decrease of μ_i), as a result, lower ionic conductivity is observed. Therefore, it can be concluded that the addition of optimum clay concentration (i.e., 5% DMMT) provides the most suitable environment for the ionic transport and achieving the highest conductivity, which is consistent with the reported one [26].

Microscopic models such as dynamic bond percolation and dynamic disorder hopping models have been proposed [27] to describe the long-range ion transport in polymer electrolytes. According to these models, the renewal time, τ_{ren}, for the segmental reorganization arising from the changes in the local geometry due to the coordination of cations with the polymer Lewis base sites, lie within the microwave range. Moreover, these models explain the frequency dependence of conductivity satisfactorily only above 100 MHz region. Hence, a physical model (i.e., jump relaxation model) was developed for structurally disordered ionic conductors [28] in order to rationalize the observed frequency dispersion. Since the dynamical effects of the polymer host due to the segmental renewing rates become less significant below microwave region. According to jump relaxation model, at very low frequencies ($\omega \rightarrow 0$) an ion can jump from one site to its neighboring vacant site successfully contributing to the dc conductivity. At higher frequencies, the probability for the ion to go back again to its initial site increases due to the short time periods available. This high probability for the correlated forward-backward hopping at higher frequencies together with the relaxation of the dynamic cage potential is responsible for the observed high frequency conductivity dispersion.

3.6. Electrical modulus analysis

The conductivity behavior in the frequency domain is more conveniently interpreted in terms of conductivity relaxation time, τ, using the representation of electrical modulus, $M^* = 1/\varepsilon^*$ [29]. The M^* representation is now widely used to analyze ionic conductivities by associating a conductivity relaxation time with the ionic process [30, 31]. In the M^* representation, a relaxation peak is observed for the conductivity process in the frequency spectra of the imaginary component of M^*. Comparison of the M^* and ε^* representations has been used to distinguish localized dielectric relaxation processes from long-range conductivity [32]. Figure 7 shows the variation of imaginary part of electrical modulus (M'') as a function of frequency for different clay concentration. The observed M'' peak in the plot is related to conuctivity relaxation of the materials. The KWW (Kohlrausch-Williams-Watts) stretched exponent function, given in Equation (7):

$$\Phi = \Phi_0 \exp\left[\left(\frac{-t}{\tau}\right)^\beta\right] \tag{7}$$

(where β is the stretching constant and τ is the characteristic relaxation time) was used to fit the M'' data. The modulus fitting was performed using the procedure of Moynihan *et al.* [29, 30] and the fitting (alogorithim) described in literature [33] was

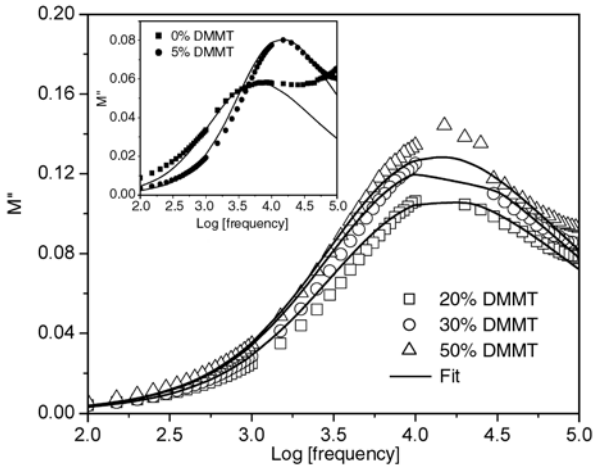

Figure 7. Imaginary part of electrical modulus (M'') vs. log(f) for different concentration of DMMT at room temperature. The continues solid line represents the fit of experimental M'' data to the decay function $\Phi = \Phi_0 \exp[(-t/\tau)^{\beta}]$.

used in our analysis. The continuous line of Figure 7 denotes the fitted value of M'' whereas the symbol corresponds to experimental data. A good agreement between the experimental data and fitted curve is evident from the figure. The value of stretching exponent parameter β, the conductivity relaxation time τ and the high frequency limit of the real part of M^* ($M_\infty = 1/\varepsilon_\infty$) obtained from the fitting are compared in Table 1 for different clay concentration. From the table it is clear that β value of the nanocomposite is always higher than that of the polymer salt complexes and the M_∞ value increases on increasing clay concentration. It is well known that β is the relaxation parameter, which increases by decreasing in the width of the relaxation time distribution.

For dielectric relaxation processes, however, relaxation peaks are observed in both M^* and ε^* representation when the two peak position in two representations are related by the ratio $\varepsilon_s/\varepsilon_\infty$ where ε_s is the static dielectric constant and ε_∞ is the dielectric constant at higher frequency limit. A comparison of the experimental data of the M^* and ε^* formalism is, therefore, useful to distinguish long-range conduction process from the localized dielectric relaxation. To visualize this, we have plotted the imaginary part of complex dielectric permittivity (ε'') and modulus (M'') as a function of frequency for 0 and 5% clay concentration of PNCEs as representative (Figure 8a) (similar behaviors are found for other compositions). Dielectric relaxation is a result of

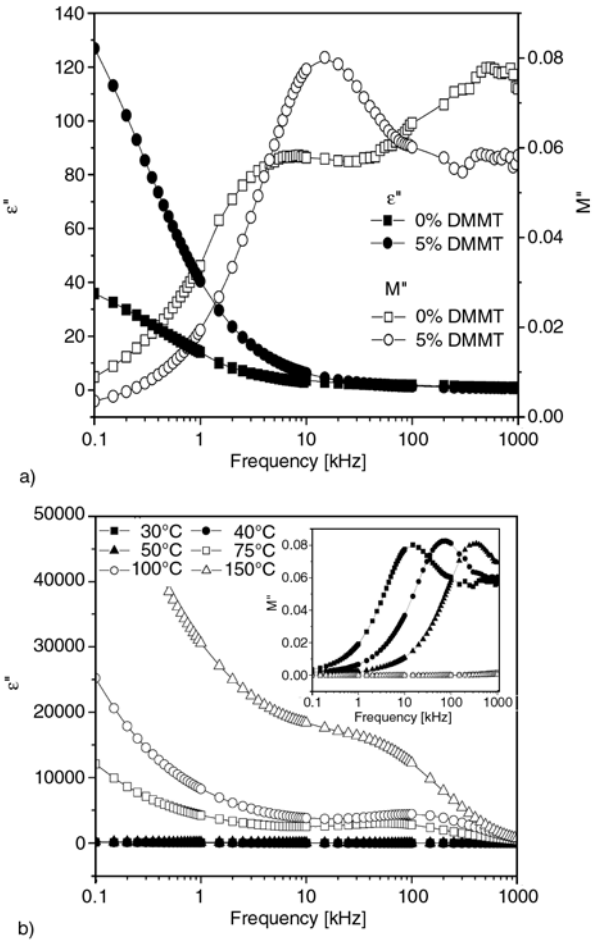

Figure 8. Variation of imaginary part of dielectric permittivity and modulus of PNCEs as a function of frequency for (a) $(PEO)_{25}$-NaI+x wt.% DMMT for x = 0% and 5% at room temperature (30°C) (b) for x = 5% at different temperatures.

the reorientation process of dipoles in the polymer chains, which show a peak in ε'' spectra. For electrolyte, with higher ion concentration the movement of ions from one site to another will perturb the electric potential of the surroundings. Motion of the other ions in this region will be affected by perturb potential. Such a cooperative motion of ions will lead to non-exponential decay, or a conduction processes with distribution of relaxation time [34]. In the imaginary part of modulus spectra a relaxation peak is observed (Figure 8a) for the conductivity processes, whereas no peak is observed in the dielectric spectra. This suggests that ionic motion and polymer segmental motion are strongly coupled manifesting as peak in the M'' spectra with no corresponding feature in dielectric spectra [35]. Similar results have been reported by Fu *et al.* [34] for PPG-$LiCF_3SO_3$ system with higher salt concen-

tration (i.e., O:Li = 30:1, 16:1, and 12:1). So the conduction in polymer electrolytes takes place through charge migration of ions between coordinated sites of the polymer along with its segmental relaxation. In addition to the main M'' peak in the low frequency region, a small peak is observed at the high frequency which is less pronounced in the 5% DMMT composite. The existence of these two peaks may be due to the heterogeneity in the texture of the polymer composites [36]. The temperature dependence of imaginary part of dielectric permittivity (ε'') and modulus (M'') as a function of frequency for x = 5% clay concentration (as representative) is shown in Figure 8b. The low frequency M'' peak shifts towards the high frequency side with rise in temperatures, but at higher temperatures we do not observe any peak. At lower temperatures, ε'' decreases on increasing frequency whereas at higher temperatures ε'' first decreases with rise in frequency (in low frequency region) followed by a peak in the loss spectra. The higher value of dielectric loss (ε'') at low frequency is due to the free charge motion within the materials. The appearance of peak is attributed to the relaxation phenomena of polymer.

4. Conclusions

The frequency dependent electrical conductivity and the associated conductivity relaxation of an ionically conducting polymer nanocomposite films was studied for different DMMT concentration. X-ray diffraction (XRD) analysis shows that the polymer-salt complexes have been intercalated into the nanometric channel of silicate layers of DMMT suggesting the formation of nanocomposites. Complex impedance analysis shows the existence of bulk and material-electrode interface properties of the nanocomposites. The electrical modulus formalism (used to describe the conductivity relaxation process), shows that the conductivity relaxation data can best be represented in terms of the stretched exponential correlation function, $\Phi = \Phi_0 \exp[(-t/\tau)^{\beta}]$. The ac conductivity spectrum obeys the universal power law in the high frequency region whereas strong low frequency dispersion was assigned to the electrode polarization effect. The conduction may be due to the drift of ions coupled to polymer segmental relaxation of polymer matrix.

References

[1] Pinnavaia T. J., Beall G. W.: Polymer-clay nanocomposites. John Wiley and Sons, New York (2001).

[2] Tjong S. C.: Structural and mechanical properties of polymer nanocomposites. Materials Science and Engineering: Reports, **53**, 73–197 (2006).

[3] Ruiz-Hitzky E.: Conducting polymers intercalated in layered solids. Advanced Materials, **5**, 334–340 (1993).

[4] Ruiz-Hitzky E., Aranada P., Casal B., Galvan J. C.: Nanocomposite materials with controlled ion mobility. Advanced Materials, **7**, 180–184 (1995).

[5] Gainnelis E. P.: Polymer layered silicate nanocomposite. Advanced Materials, **8**, 29–35 (1996).

[6] MacCallum J. R., Vincent C. A.: Polymer electrolyte review-I. Elsevier, London (1987).

[7] Meyer W. H.: Polymer electrolytes for lithium-ion batteries. Advanced Materials, **10**, 439–448 (1998).

[8] Gray F. M: Polymer electrolytes. The Royal Society of Chemistry, Cambridge (1997).

[9] Fauteux D., Lupien M. D., Robitaille C. D.: Phase diagram, conductivity and transference number of PEO-NaI electrolyte. Journal of the Electrochemical Society, **134**, 2761–2767 (1987).

[10] Rietman E. A., Kaplan M. L., Cava R. J.: Lithium ion-poly(ethylene oxide)complexes. I. Effect of anion on conductivity. Solid State Ionics, **17**, 67–73 (1985).

[11] Bruce P. G.: Solid state electrochemistry. Cambridge University Press, Cambridge (1995).

[12] Sinha Ray S., Okamoto M.: Polymer/layered silicate nanocomposites: A review from preparation to processing. Progress in Polymer Science, **28**, 1539–1641 (2003).

[13] Ratna D., Divekar S., Samui A. B., Chakraborty B. C., Banthia A. K.: Poly(ethylene oxide)/clay nanocomposite: Thermomechanical properties and morphology. Polymer, **47**, 4068–4074 (2006).

[14] Thakur A. K., Pradhan D. K., Samantaray B. K., Choudhary R. N. P.: Studies on an ionically conducting polymer nanocomposite. Journal of Power Sources, **159**, 272–276 (2006).

[15] Pradhan D. K., Samantaray B. K., Choudhary R. N. P., Thakur A. K.: Effect of plasticizer on structure-property relationship in composite polymer electrolyte. Journal of Power Sources, **139**, 384–393 (2005).

[16] Chen H-W., Lin T-P., Chang F-C.: Ionic conductivity enhancement of the plasticized PMMA/$LiClO_4$ polymer nanocomposite electrolyte containing clay. Polymer, **43**, 5281–5288 (2002).

[17] Cameron G. G., Ingram M. D., Qureshi M. Y., Gearing H. M., Costa L., Camino G.: The thermal degradation of poly(ethylene oxide) and its complexes with NaCNS. European Polymer Journal, **25**, 779–784 (1989).

[18] Shen Z., Simon G. P., Cheng Y-B.: Saturation ratio of poly(ethylene oxide) to silicate in melt intercalated composite. European Polymer Journal, **39**, 1917–1924 (2003).

[19] Macdonald J. R.: Impedance spectroscopy, emphasizing solid materials and systems. Wiley, New York (1987).
[20] Dias F. B., Batty S. V., Voss J. P., Ungar G., Wright P. V.: Ionic conductivity of a novel smectic polymer electrolyte. Solid State Ionics, **85**, 43–49 (1996).
[21] Qian X., Gu N., Cheng Z., Yang X., Wang E., Dong S.: Plasticizer effect on the ionic conductivity of PEO-based polymer electrolyte. Materials Chemistry and Physics, **74**, 98–103 (2002).
[22] Kanapitas A., Pissis P., Kotsilkova R.: Dielectric studies of molecular mobility and phase morphology in polymer-layered silicate nanocomposites. Journal of Non-Crystalline Solids, **305**, 204–211 (2002).
[23] Jonscher A. K.: Dielectric relaxation in solids. Chelsea Dielectric Press, London (1983).
[24] Jonscher A. K.: The universal dielectric response. Nature, **267**, 673–679 (1977).
[25] Mauritz K. A.: Dielectric relaxation studies of ion motion in electrolyte-containing perfluorosulfonate ionmres. 4. Long range ion transport. Macromolecules, **22**, 4483–4488. (1989).
[26] Chen H-W., Chiu C-Y., Wu H-D., Shen I-W., Chang F-C.: Solid-state electrolyte nanocomposites based on poly(ethylene oxide), poly(oxypropylene)diamine, mineral clay and lithium perchlorate. Polymer, **43**, 5011–5016 (2002).
[27] Ratner M. A., Shriver D. F.: Ion transport in solvent free polymers. Chemical Reviews, **88**, 109–124 (1988).
[28] Funke K.: Jump relaxation in solid electrolytes. Progress in Solid State Chemistry, **22**, 111–195 (1992).
[29] Macedo P. B., Moynihan C. T., Bose R.: Role of ionic diffusion in polarization in vitreous ionic conductors. Physics and Chemistry of Glasses, **13**, 171–179 (1972).
[30] Moynihan C. T., Boesch L. P., Laberge N. L.: Decay function for the electric field relxation in vitreous ionic conductors. Physics and Chemistry of Glasses, **14**, 122–125 (1973).
[31] Angell C. A.: Dynamic processes in ionic galsses. Chemical Reviews, **90**, 523–542 (1990).
[32] Gerhardt R.: Impedance and dielectric spectroscopy revisited: Distinguishing localized relaxation from long-range conductivity. Journal of Physics and Chemistry of Solids, **55**, 1491–1506 (1994).
[33] Baskaran N.: Conductivity relaxation and ion transport processes in glassy electrolyte. Journal of Applied Physics, **92**, 825–833 (2002).
[34] Fu Y., Pathmanathan K., Stevens J. R.: Dielectric and conductivity relaxation in poly(propylene oxide)-lithium triflate complexes. The Journal of Chemical Physics, **94**, 6323–6329 (1991).
[35] Jeevanandam P., Vasudevan S.: Arrhenius and non-Arrhenius conductivities in intercalated polymer electrolytes. Journal of Chemical Physics, **109**, 8109–8117 (1998).
[36] Chanmal C. V., Jog J. P.: Dielectric relaxations in PVDF/$BaTiO_3$ nanocomposites. Express Polymer Letters, **2**, 294–301 (2008).